

Flexible and biocompatible polypropylene ferroelectret nanogenerator (FENG): On the path toward wearable devices powered by human motion

Wei Li^a, David Torres^b, Tongyu Wang^b, Chuan Wang^b, Nelson Sepúlveda^{a,b,*}

^a Department of Mechanical Engineering, Michigan State University, East Lansing 48824, USA

^b Department of Electrical and Computer Engineering, Michigan State University, East Lansing, MI 48824, USA

ARTICLE INFO

Keywords:

Nanogenerators
Polypropylene ferroelectrets
Mechanical energy harvesting
Energy storage
Self-powered devices

ABSTRACT

Recently, there has been tremendous research efforts on the development of energy harvesters that can scavenge energy from ubiquitous forms of mechanical energy. The most studied mechanisms are based on the use of piezoelectric and triboelectric effects. Polypropylene ferroelectret (PPFE) is introduced here as the active material in an efficient, flexible, and biocompatible ferroelectret nanogenerator (FENG) device. PPFE is charged polymers with empty voids and inorganic particles that create giant dipoles across the material's thickness. Upon applied pressure, the change in the dipole moments generate a change of the accumulated electric charge on each surface of the PPFE film, resulting in a potential difference between the two electrodes of the FENG. The mechanical-electrical energy conversion mechanism in PPFE films is described by finite element method (FEM). Further investigation of the developed device shows that the magnitudes of the generated voltage and current signals are doubled each time the device is folded, and an increase with magnitude or frequency of the mechanical input is observed. The developed FENGs is sufficient to light 20 commercial green and blue light-emitting diodes (LEDs), and realize a self-powered liquid-crystal display (LCD) that harvests energy from user's touch. A self-powered flexible/foldable keyboard is also demonstrated.

1. Introduction

Harvesting energy from our natural environment has been the focus of multiple research efforts in the past decades. Progress in this field has far-reaching implications for the growing environment problems resulting from greenhouse gas emission of fossil fuels. Furthermore, advances in portable energy scavenging devices will shed light on the development of self-powered and autonomous electronics; which will impact a broad range of applications in wireless sensors, biomedical implants, infrastructure monitoring, and portable/wearable electronics [1–5]. Although mechanical energy is ubiquitous in our daily life, it was not until recently that this form of energy began to be scavenged from low energy density environments. Mechanical energy is present day and night and it can be found in tiny and sometimes even unnoticed forms, e.g. gentle wind breeze [6–10], water waves [11–14], rotating tires [15–17], walking [18–20], and keyboard typing [21]. Even simple body movement [22–24] or biological functions (e.g. heartbeats or diaphragm activities [25–29]) involve mechanical energy that has recently been tapped as renewable energy sources.

Personal electronics are advancing toward an era where the pursuit of multifunctionality and wearability has become an important trend

[30–35]. Similarly to the recent developments in flexible light-emitting diodes (LEDs), artificial skin, and stretchable electronics [36–42], devices designed to harvest small sources of mechanical energy should address the issues of lightweight, flexibility, and biocompatibility. This will make the technology to be portable and compatible with smart electronics [30,43–45], ultimately defining the path toward self-powered wearable devices. The prevailing mechanisms of thin film-based mechanical energy harvesting have been limited to conversion based on piezoelectric effect [46–48]. Recently, Wang and co-workers revolutionized the field by inventing triboelectric nanogenerators (TENGs) which are capable of generating very high voltages [49]. Their work is continuously advancing to further enhance efficiency of TENGs [50–52].

In this work, we introduce a different operating mechanism to the field of flexible thin film nanogenerators (NGs) based on polypropylene ferroelectret (PPFE) which harvest mechanical energy from human motion. We demonstrate flexible, foldable, biocompatible, highly efficient thin film ferroelectret nanogenerators (FENGs). The devices comply with the flexibility, wearability, lightweight, and portability demands mentioned earlier. A FENG with surface area more than 300 cm² is demonstrated in this paper by using bar-coating technique

* Corresponding author at: Department of Mechanical Engineering, Michigan State University, East Lansing 48824, USA.
E-mail address: nelsons@egr.msu.edu (N. Sepúlveda).

[53]; they can also be folded to sizes smaller than 1 cm^2 and generate higher electric potentials. Furthermore, their simple fabrication allows for encapsulated low-cost devices. In view of the environment, health, and safety [2], the fabrication of encapsulated FENG avoids the use of harmful elements (e.g. lead) or toxic materials (e.g. carbon nanotubes), making it more attractive for biocompatible and perhaps even implantable applications. Through finite element method (FEM), the mechanical-electrical energy conversion mechanism of FENG was studied; and the relationship between internal stress, change of electric field, and charge transport are investigated. Due to its thin film structure, the device can be bent or even folded easily. Further experiments show that both the open-circuit voltage (V_{oc}) and short-circuit current (I_{sc}) are doubled with each folding along an axis of symmetry. Since V_{oc} and I_{sc} are doubled with each folding action, the output power of the FENG can be easily and significantly increased. We also study the electrical output produced by the device for time-dependent mechanical input. Additionally, device electrical output for different pressure input magnitudes (while keeping the frequency constant), and for different frequencies (while keeping the magnitude constant) are investigated. The results revealed the frequency- and pressure-dependent properties of the developed device. Finally, we developed FENG-based systems for three niche applications: 1) Illumination: we demonstrate that the energy harvested by a stacked FENG ($60\text{ mm}\times 60\text{ mm}$, 7 layers) is able to power 20 commercial green and blue LEDs connected in series; 2) Self-powered touch liquid crystal display (LCD): this touch screen scavenges energy from finger touch to supply power during operation; and 3) Flexible/foldable keyboard: this thin film-based keyboard is powered by harvested energy from each keystroke, and its size can be reduced by simple folding, thus enabling portability.

2. Methods

2.1. Fabrication of polyimide (PI) encapsulated FENG

By using sputter coater (Hummer X, Anatech Inc.), a rectangular thin layer of silver (500 nm) was deposited on a PPFE (EMFIT Corporation) film (80 μm) via shadow mask. With the electrode connection covered by a small piece of PTFE film (4 mm \times 4 mm), a layer of PI (PI-2525, HD MicroSystem) is spin-coated at 2000 rpm for 1 min. The PTFE tape was removed after spinning, leaving the contact pads for electrode exposed. After curing the PI at a temperature of 100 $^\circ\text{C}$ for 5 min, the PI layer was peeled off with help of a blade. Then, the sample was flipped, followed by sputtering another layer of silver (500 nm) on the backside of PPFE using the same shadow mask. After covering the electrode area with PTFE film (4 mm \times 4 mm), another layer of PI is spin-coated at 2000 rpm for 1 min. The PTFE film was removed and the wafer was then cured at 100 $^\circ\text{C}$ for 90 min, followed by peeling off with the help of blade. The last step was connecting two copper wires to the two exposed electrode pads via copper tape.

2.2. Fabrication of flexible FENG keyboard

A layer of electric paint (Bare Conductive inc.) with the area of 175 mm \times 75 mm is coated on a layer of PPFE film by bar-coating technique. A wire-wound (3/8'' \times 16'') lab rod with a glass drawdown plate (R.D. Specialties, Inc.) is used. After cured at room temperature for 15 min, coated PPFE film is flipped and a second layer of electric paint is bar-coated via a lattice mask which was firmly attached to the PPFE film, followed by curing for 15 min. Then, gold wires with diameter of 31.75 μm are connected to the keys which were defined by the patterned shadow mask. Keyboard stickers were attached to the other side.

2.3. Tests and measurements

In the V_{oc} measurement process, the FENGs were connected to a low-noise nanovoltmeter (Keithley 2182A). The I_{sc} signal was measured by a low-noise picoammeter (Keithley 6487). The linear moving stage was driven by a large holding torque (1.9 Nm) stepper motor (Nema, Inc) via a ballscrew, and controlled by an Integrated 400 MHz real-time controller (cRIO-9075, National Instruments) with an analog output module (NI 9263, National Instruments). The output signal of flexible FENG keyboard were acquired by cRIO-9075 with an analog input module (NI 9201, National Instruments)

3. Results and discussion

Polypropylene (PP) foams are good thermal insulators with a high mechanical strength-to-weight ratio. The active material in the developed FENGs are prepared by starting with PP film containing tiny foreign inorganic particles (e.g. silicates). When the film experiences stretching in two perpendicular directions, the inorganic particles serve as a stress concentrator or microcracks resulting in lens-shaped voids in the PP film. During this process, high pressure (e.g. 5 MPa) nitrogen or carbon dioxide diffuse into the film which is full of voids, so that the internal pressure within the voids becomes equal to the external pressure. Subsequently, the external gas pressure is suddenly released, resulting in dramatically swell of those voids in PP film. For the purpose of stabilizing and stiffening the swelling voids at room temperature, thermal treatment (usually higher than 100 $^\circ\text{C}$) is carried out to increase the crystallinity of the polymer matrix [54–56].

Unlike ferroelectric materials which have a spontaneous electric polarization, PP films are completely nonpolar materials unless the internal voids are charged by dielectric barrier microdischarges [55,57]. By means of plasma discharges in the voids of PP foam, completely non-polar materials without any molecular dipole can behave like ferroelectrics. Although the PPFE would exhibit the same macroscopic behavior as traditional well-known piezoelectric polymers or piezocomposite [53,58], their microscopic operating principles are different. For β -phase polyvinylidene fluoride (PVDF), which is the most commonly used piezopolymer in electromechanical devices [59], the hydrogen atoms have net positive charge and the fluorine atoms have net negative charge (Fig. 1a). The lattice parameters of β -phase PVDF are $a=8.64\text{ \AA}$, $b=4.82\text{ \AA}$ and $c=2.64\text{ \AA}$ [60], whereas the dipole dimensions in the PPFE are determined by the sizes of the charged voids. By applying a large electric field to the PP film, Paschen-breakdown occurs inside the voids [55]. The current within the air gap transfers a sheet charge density across the air gap (Fig. 1b). During microplasma discharges, charges separated by the ionization of the gas transportation under the charging field, and light flashes can be observed with the naked eye. PP foam is full of artificial voids with different size, ranging from $\sim 1\text{ }\mu\text{m}$ scale to $\sim 100\text{ }\mu\text{m}$ scale, which form highly oriented giant dipoles. If two conductive layers are deposited on the surfaces of the PPFE film, which functions as electrodes, then the giant dipoles in the PPFE induce charge of opposite polarity in each electrode. The charged voids change their thickness and thus their dipole moments upon application of mechanical stress (Fig. 1c), i.e. compressing PPFE film will result in smaller dipoles moments. The change of dipole moments is capable of driving the electrons from the electrode with negative charge to the electrode with positive charge, generating a difference in potential between the electrodes (generated voltage under open circuit condition) or flow of charge from one electrode to the other (generated current under short circuit condition). This macroscopic behavior of PPFE films is very similar to that of well-known solid piezoelectric crystals, even though the microscopic origins of the observed phenomena are different. By comparison with traditional piezoelectric materials, PPFE films features with flexibility and internally charged cellular structures, which makes them highly efficient in charge storage and more sensitive to mechanical stress.

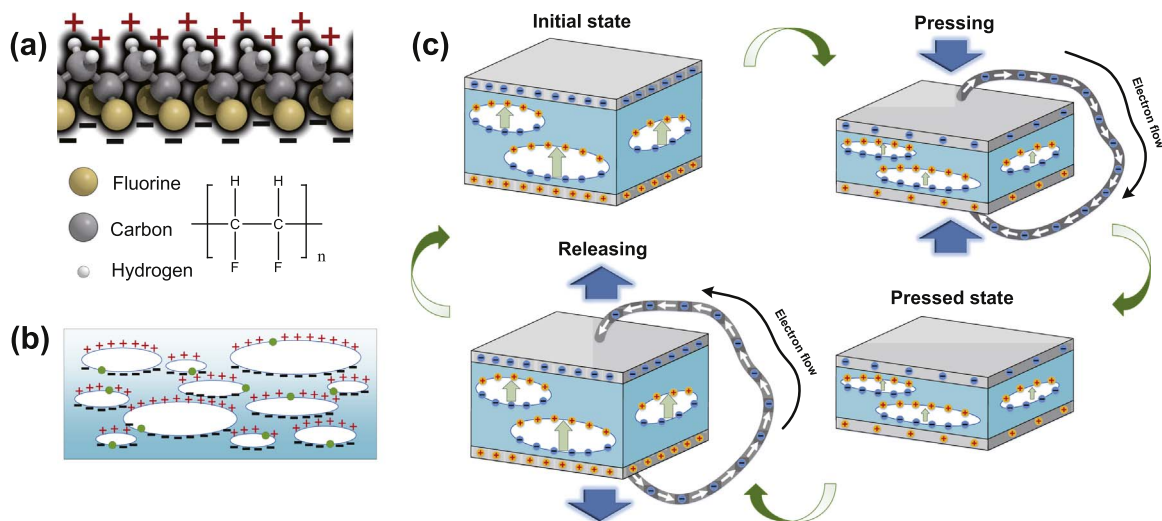


Fig. 1. Schematic illustration of the operating principle of the FENGs. (a) Molecular structure of piezoelectric β -phase polyvinylidene fluoride (PVDF). (b) Bipolar voids and charge distribution of PPFE after microplasma discharging, showing that the upper and lower surfaces of the voids are oppositely charged. Green spheres indicate foreign particles that facilitate void formation. (c) Illustrative schematic of a press-release cycle and corresponding dipole and charge dynamics of FENGs.

More importantly, PPFE films have significantly greater piezoelectric coefficient ($d_{33} \sim 400$ pC/N) than typical piezopolymers like PVDF ($d_{33} \sim 15$ pC/N) [61], and parylene-C ($d_{33} \sim 2$ pC/N) [59].

The FENG is a sandwich-like metal-insulator-metal (MIM) structure which makes easy large-scale fabrication. The fabrication process of a FENG with an area of (35 mm \times 25 mm) encapsulated by PI films is illustrated in Fig. 2a. A PPFE film fabricated by EMFIT Corporation with a nominal thickness of 80 μ m and piezoelectric coefficient $d_{33} \sim 400$ pC/N serves as the insulator, and two thin silver films (500 nm in thickness) sputtered on the both sides of PPFE act as metal electrodes. Copper wires are fixed on the electrodes by using conductive paint and copper tape, providing electrical terminals that allowed for external circuitry connections to the FENG. Due to the outstanding reliability, durability, mechanical and chemical properties, two thin spin-coated PI films serve as encapsulation layers that protect the FENG device from invasive chemicals and provide mechanical robustness. It has been demonstrated that encapsulation of a flexible device with biocompatible PI films isolates the functional part of the device from bodily fluids and tissue, thus minimizing the risks of failure or immune response in bioimplantable applications [25]. Furthermore, PI encapsulation layer revealed no evidence of toxicity from *in vitro* studies with human epithelial keratinocytes [27]. Fig. 2b provides an exploded-view schematic diagram of the fabricated FENG. A scanning electron microscopy (SEM) image of the cross-section of PP foam and an optical image of the FENG appear in Fig. 2c and d, respectively. The use of backscattered electrons reveals good contrast and clear definition of the structure of PPFE foam film. Since the production of backscattered electrons is strongly dependent on the average atomic number of the sample, silicate particles appeared to be much brighter than their surrounding PP cellular film. The SEM image also clearly shows the bipolar voids described earlier. Fig. 2e and f show SEM images of the surface of the PPFE foam, using secondary and back-scattered electrons, respectively. The voids in the PP foam can be identified at the dark regions in Fig. 2f, where lower material density produces fewer backscattered electrons.

In order to obtain a more quantitative characterization of the energy generating ability of FENG, the electric potential and electric field distribution inside the FENG is analyzed by FEM (COMSOL Multiphysics 5.2). The model describes the charge transfer between two electrodes and it represents the first FEM model for a PPFE-based energy harvester. Fig. 3a illustrates a schematic diagram of the constructed model. A 2-D section of FENG (80 μ m \times 300 μ m) is filled with seven voids with different shapes and sizes and two silver

electrodes (10 μ m \times 300 μ m). The surface charge densities on the top and bottom surfaces of each void are set to 10^7 C/m² and -10^7 C/m², respectively. Both silver electrodes are set to an electric potential of 0 V (i.e. they are grounded). Figs. 3b and c show the calculated electric potential and electric field distribution inside the section without external pressure, respectively. It can be seen that due to the charged surfaces of each void inside the section, there is an electric potential across the surfaces of the voids as well as between them. Fig. 3d and e show the simulated resulting electric potential and electric field distribution when 1 MPa pressure is applied vertically to the upper surface of the film. The geometric shape of voids along with the electric potential and electric field distribution are changed due to the applied external pressure. The size, shape, and density of the voids determine the vertical stiffness of FENG, which plays an important role in its mechanical-electrical conversion ability [62–64]. Fig. 3f shows charge density distribution of the upper and lower surfaces before and after external pressure is applied. As can be seen, the upper surface accumulates negative charge while lower surface accumulates positive charge; and the shape of the charge distributions for both surfaces are the same due to the geometric symmetry of the model. Once the external pressure is applied to the upper surface, the charge distribution shape at both surfaces remains; but the absolute values of the accumulated charge at both surfaces decreased. When both electrodes are grounded, the negative charge on the upper electrode and positive charge on the lower electrode flow to ground simultaneously. When both electrodes are left floating, the accumulation of different charge between electrodes produces a difference in potential. By applying gradually increasing pressure on the upper surface of the model and integrating the surface charge density of upper and lower electrodes, the relationship between the total charges accumulating on both electrodes and the vertical pressure can be obtained (Fig. 3g). It can be seen that the accumulated charge on both electrodes decreases proportionally with applied pressure. This “macroscopic” behavior of FENG resembles that of traditional piezoelectric materials.

To investigate the performance of the FENG, V_{oc} and I_{sc} generated during periodical external pressure and release are measured. The pressure is provided by a stepper motor with 1.9 Nm holding torque via a linear motion stage (Fig. 4a and b). The pressing stage is mounted on an optical table for vibration isolation and with good electrical grounding. Fig. 4c and d show the measurement results of the FENG with actual force contact area of 15 mm \times 15 mm. A low noise nanovoltmeter and a low noise picoammeter were used to measure the V_{oc} and I_{sc} , respectively. It can be seen that the device exhibits typical

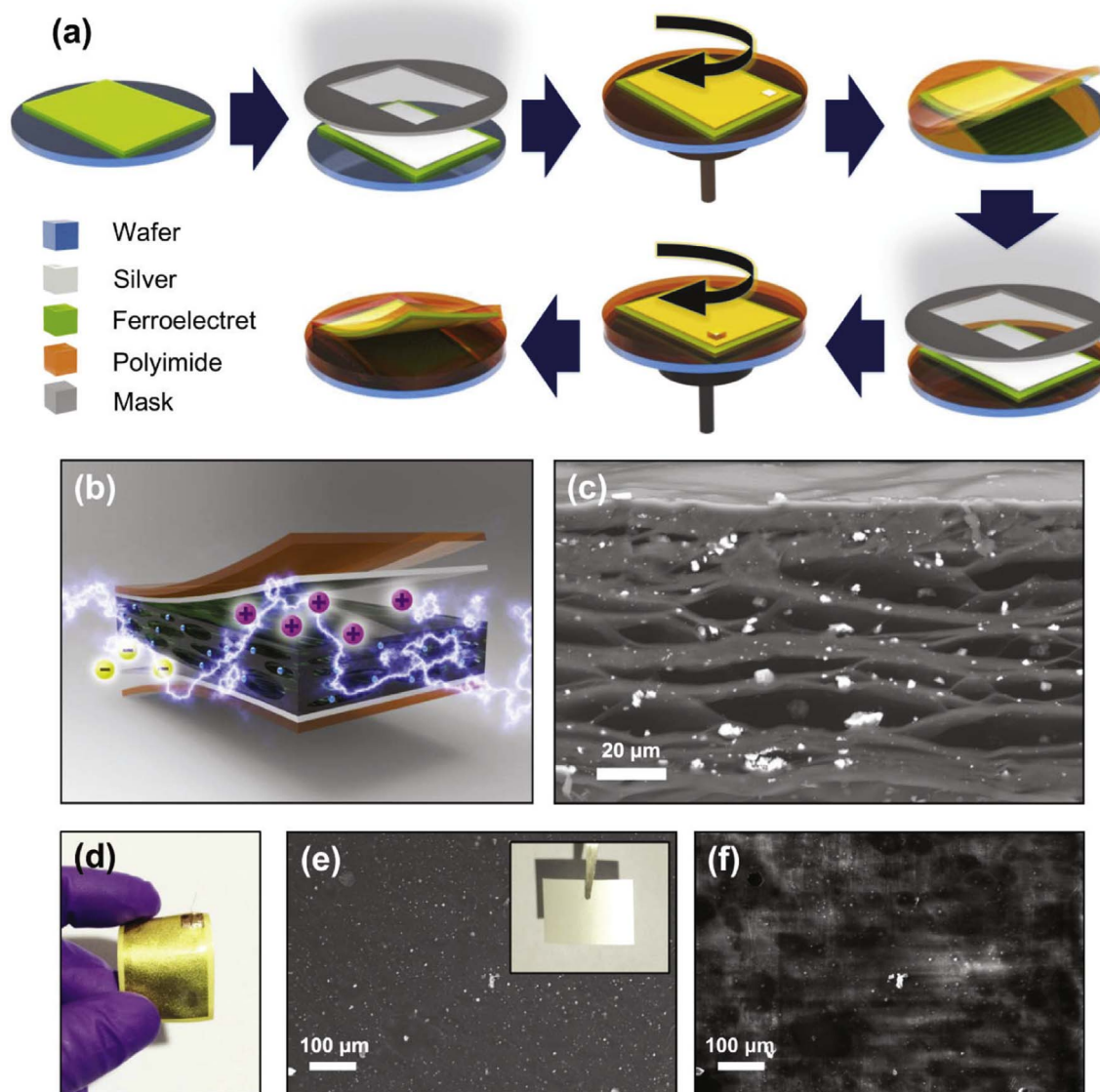


Fig. 2. Fabrication of encapsulated biocompatible and flexible thin film FENG. (a) Schematic illustration of the fabrication process of FENG. (b) Exploded-view illustration of the encapsulated FENG, which consists of a stacked metal-PPFE-metal structure without moving parts or microfabricated features. (c) Cross-sectional backscattered electron SEM image of the PP foam, showing the cellular structure and silicate particles (brighter areas in the image). (d) Photograph of the fully encapsulated FENG bent by fingers. (e) Secondary electron SEM image of the surface of PPFE and the photograph of PPFE (inset). (f) Backscattered electron SEM image of the same area of (e). The darker regions corresponds to voids below the film's surface.

piezoelectric-like behavior; i.e. when the FENG is pressed by the linear stage, V_{oc} and I_{sc} increase dramatically, and when the external pressure is released both signals experience very similar change, but with opposite sign. The measured peaks for V_{oc} and I_{sc} are ~ 1 V and ~ 0.1 μ A, respectively. The switching polarity test [34] was carried out to confirm that the measured output signals are generated by the FENG rather than artifacts caused by the measurement instruments themselves (See [Movie S1, Supporting Information](#)).

The influence of the geometric form of FENG on the output electric signals is investigated. In order to increase the mechanical-electrical transformation efficiency of FENG, we folded the fabricated device along an axis of symmetry (Fig. 5a). When the film is folded once, the magnitudes of both V_{oc} and I_{sc} are doubled, which is tantamount to doubling the piezoelectric coefficient d_{33} of the unfolded state. When the FENG is folded three times, the measured electric signals are about 8 times as high as that of the unfolded state, suggesting that the output magnitude of V_{oc} and I_{sc} of FENG follows a 2^n relationship, where “ n ” represents the number of folds along an axis of symmetry. This

suggests that the generated charge on the surface of PPFE is proportional to the pressured area, which increases by 2^n during the folding process. Hence, the mechanical-electric transformation efficiency of the FENG can be significantly enhanced by simple folding. This allows for the use of a simple and low-cost bar-coating techniques (Fig. 5b) to form electrodes at both surfaces of a PPFE film, so as to fabricate FENG with adjustable performance, overcoming the size limitation of the FENG caused by chamber growth and complicated transfer process [53]. Two layers of electrically conductive paint (Bare Conductive Inc.) were coated onto the PPFE film by using 3/8'' \times 16'' wire wound lab rod with wet film thickness of 25.6 μ m. A large-area FENG with dimensions of 180 mm \times 180 mm was fabricated (Fig. 5c). It is also possible to increase the output of the FENG by stacking single layers of PPFE separated by a conductive layer, to form a multi-layer structure where the giant dipoles in the adjacent film have opposite orientation. The surface of each single film having the same polarity are electrically connected in parallel to form a multi-layer device (Fig. 5d and e). It is noted that the increase in mechanical-electrical transformation effi-

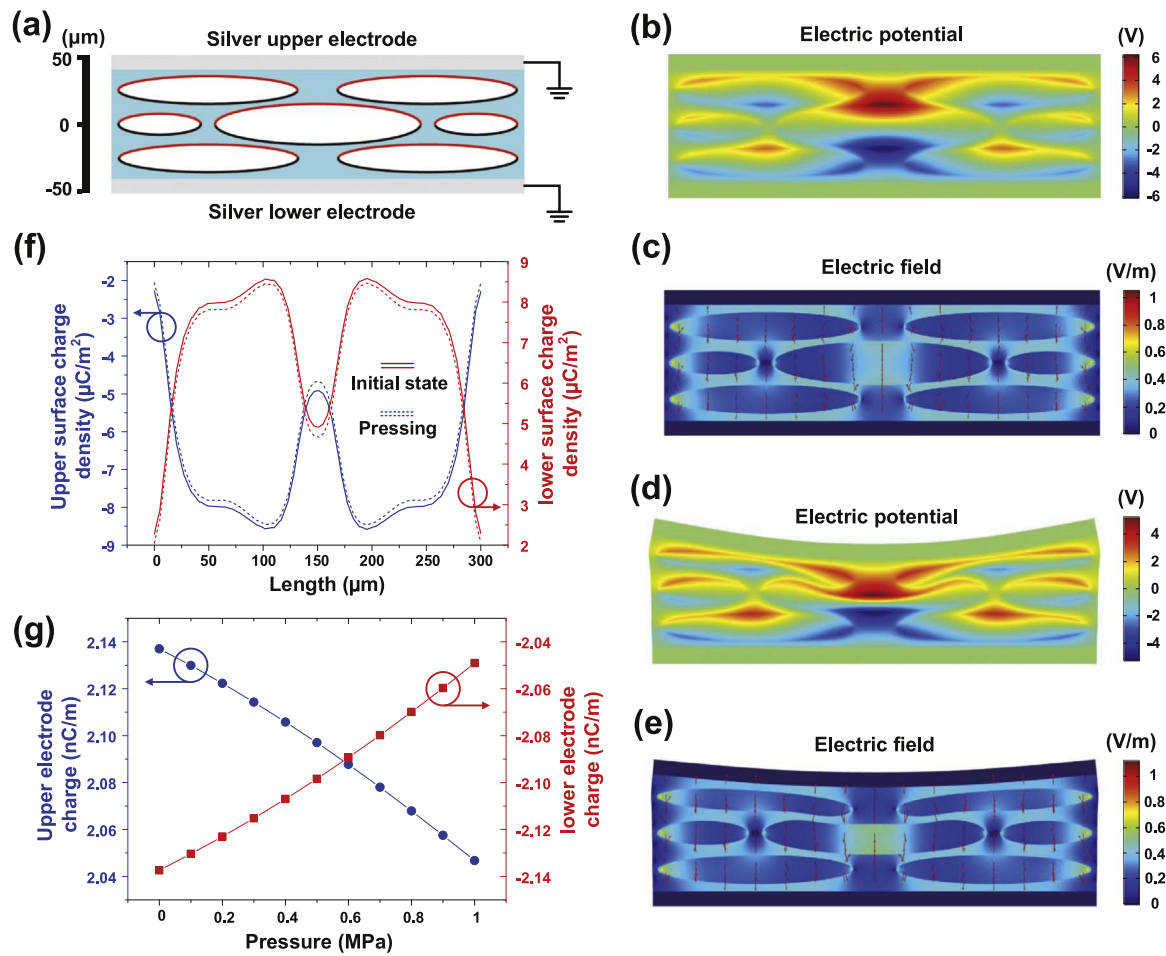


Fig. 3. Theoretical model and study of FENGs by FEM calculation. (a) Schematic model of a section of FENG (80 $\mu\text{m} \times 300 \mu\text{m}$). Simulation results of (b) electric potential distribution and (c) electric field distribution of the model without external pressure. Red arrows represent electric field vectors. Simulation results of (d) electric potential distribution and (e) electric field distribution of the model under 1 MPa pressure applied to the top surface. (f) Charge density distribution of the upper and lower surfaces before and after external pressure is applied. (g) Relationship between total accumulated charge at the upper and lower electrodes with applied pressure.

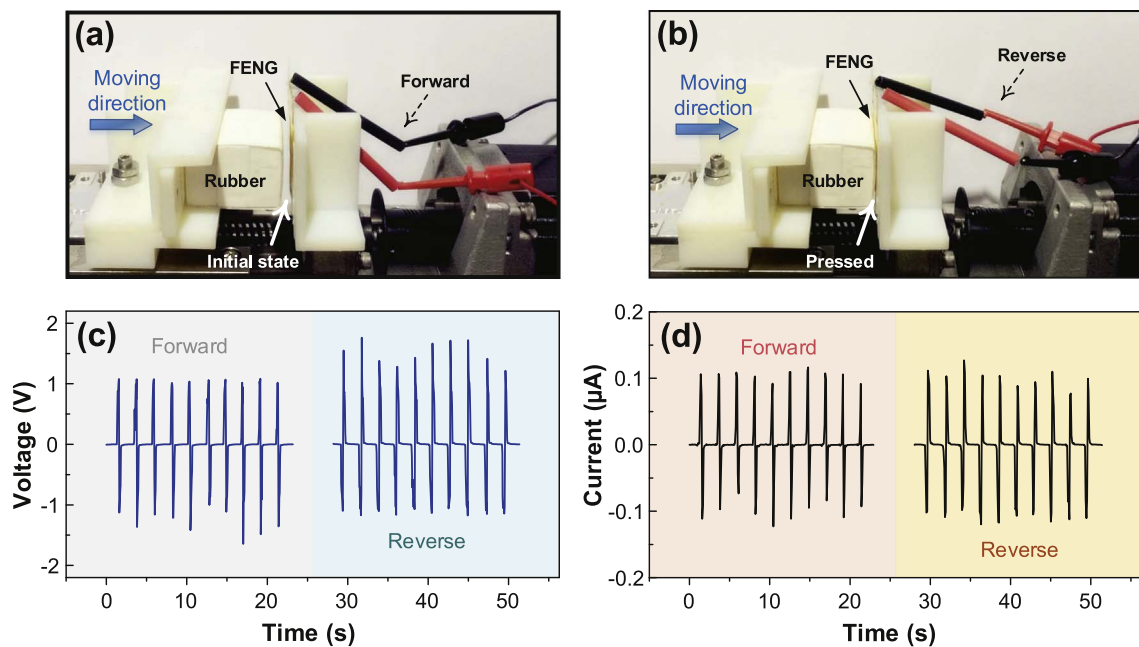


Fig. 4. Photographs of mechanical loading test of FENG at (a) initial state while the electrodes are connected forward, and (b) pressed state while the electrodes are connected reverse. The FENG is fixed, and a step motor applies a pressure perpendicular to the FENG. The pressure applied to the FENG is real-time controlled. This set-up is also used to perform the pressure-dependent and frequency-dependent experiments discussed in this work. Experimental results of (c) V_{oc} and (d) I_{sc} of the FENG. Different sign in output for pressing-releasing sequence is observed when the electrical connections to the FENG are reversed.

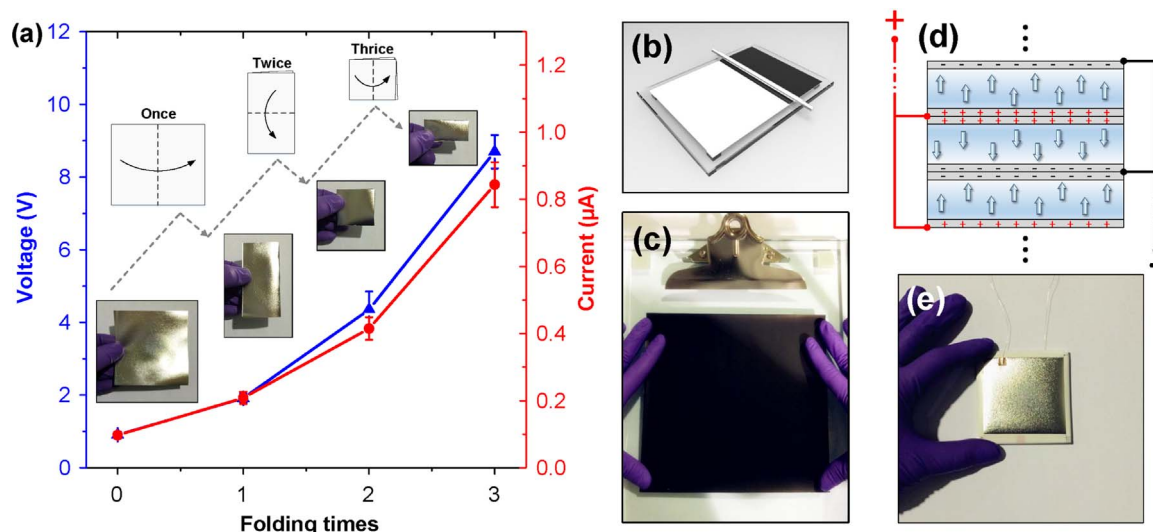


Fig. 5. Performance of FENG with folding: (a) Output voltage and current signals are amplified with each folding action along an axis of symmetry. The performance follows a 2^n behavior, where n is the number of folds. (b) Convenient bar-coating process for fabricating electrodes over large-area PPFes. (c) Large-area FENG fabricated with simple bar-coating technique. (d) Schematic illustration and (e) photograph of stacked FENG ($\sim 40 \text{ mm}^2$) to increase magnitude of the generated electric signals. Common electrical contacts are made on alternating metal layers.

ciency by stacking single layers of PPF (See [Movie S2, Supporting Information](#)) follows the same rationale of the symmetric folding process regardless of how you fold the film, the surfaces with the same polarity are always in electric contact. This folding characteristic of the FENG not only demonstrates a practical, flexible, and easy way to improve its performance, but also confirms the linear superposition behavior [65] of FENG; which also validates the macroscopic piezoelectric behavior of the material.

Further characterization of the FENG was made by measuring the FENG's response for an oscillatory input as a function of frequency and magnitude. [Fig. 6a–c](#) shows the stage moving displacement, V_{oc} , and

I_{sc} as a function of time of a FENG under pressing with frequencies of 1 Hz, 0.5 Hz, and 0.25 Hz. The tested FENG is periodically pressed by the real-time controlled motorized stage, which controlled the lateral displacement of a rubber cuboid parallel to the FENG surface (see [Fig. 4](#)). It can be seen that increasing the frequency with the same load amplitude increases both V_{oc} and I_{sc} generated by FENG, similar to the phenomenon observed from piezoelectric based NGs [25]. [Fig. 6d–e](#) show the V_{oc} , and I_{sc} as a function of time of a FENG under different stage displacement (3 mm, 1.5 mm, and 0.75 mm), which corresponds to different pressures applied on the device. It can be seen that the amplitude of both V_{oc} and I_{sc} is proportional to the stage moving

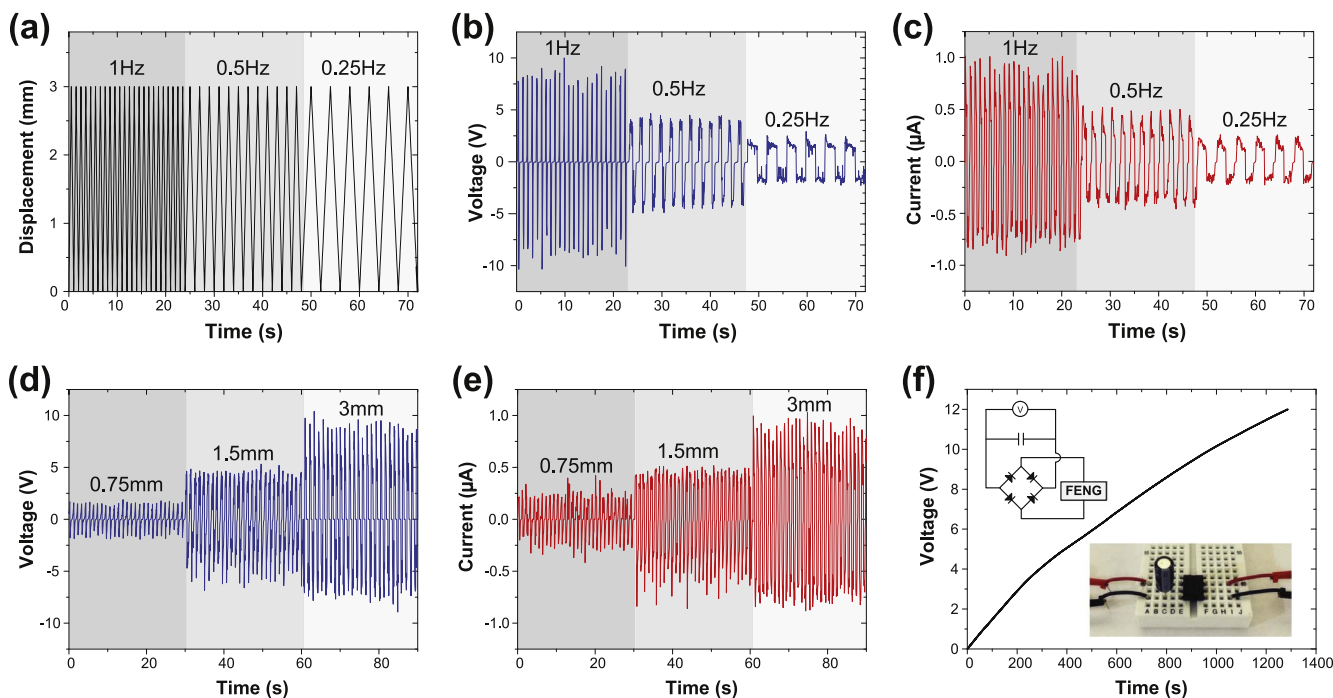


Fig. 6. Time and magnitude response of FENG. (a) Displacement of linear stage controlling the pressure on a FENG as a function of time. Three different displacement frequencies (1, 0.5, and 0.25 Hz) with same magnitude (3 mm) were used. (b), (c) Corresponding V_{oc} and I_{sc} generated from FENG. Magnitude of voltage and current peaks decrease with frequency. (d), (e) V_{oc} and I_{sc} generated from FENG for linear stage input of different displacements (i.e. different pressure magnitudes input) and same frequency (1 Hz). (f) Plot of voltage stored in a $22 \mu\text{F}$ capacitor for a FENG under a periodic input (3 mm, 1 Hz) as a function of time. The maximum voltage that can be read by the nanovoltmeter was 12 V. Inserts in the plot show the electrical schematic of the circuit used and a photograph of the implemented circuit.

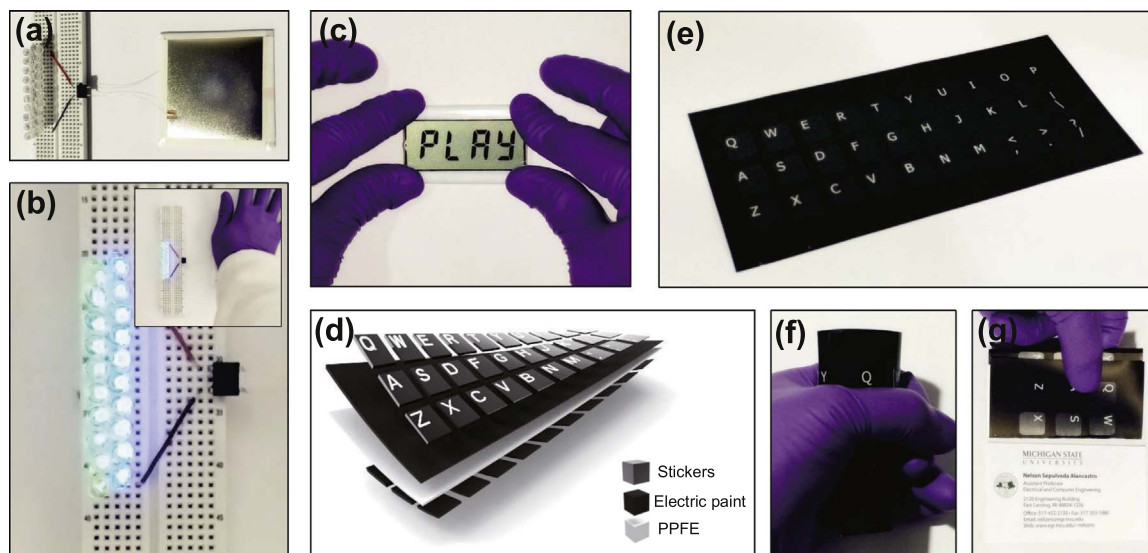


Fig. 7. Applications of FENG for versatile mechanical energy harvesting. (a) A FENG consisting of a stack of 7 PPFE film layers connected to 20 green and blue commercial LEDs through a rectifier. (b) LEDs connected are lit by FENG just by one time hand-press. (c) A self-powered LCD touch screen which is able to scavenge energy from finger touch. Word “PLAY” is displayed on the screen by touching a small area of the corners by the user. Exploded view (d) and photograph (e) of developed FENG-based flexible/foldable self-powered keyboard. Rollability and foldability of the developed keyboard is shown by (f) rolling it with hand or (g) folding it to the size of a business card.

displacement or the applied pressure. To demonstrate the energy harvesting capability of the device, a Schottky bridge rectifier (DB102, RECTRON Inc.) is connected between the FENG and a low leak capacitor (22 μF , 50 V, Nichicon) (Fig. 6f). The nanovoltmeter is used to measure the voltage across the capacitor. In this configuration, the voltage generated by the FENG (during pressing and releasing) is used to charge the capacitor. It can be seen that the stored voltage increases continuously with each cycle of loading and releasing process. As the process continues, the stored voltage keep increasing to a maximum magnitude determined by the range of nanovoltmeter. According to the charging curve of Fig. 6f, it can be anticipated that the stored voltage has the trend to continue increasing for even higher values (the maximum stored energy will be ultimately determined by the capacitor). This demonstrates that the FENG could be integrated into autonomous electronic systems where harvested energy is used, for example, to charge a solid-state battery.

To demonstrate that the harvested energy can be utilized as an effective power source, a FENG consisting of a stack of 7 PPFE film layers is used to provide energy for commercial LEDs. Fig. 7a shows the device is connected with a Schottky bridge rectification circuit and 20 LEDs (green and blue, 3.0–3.4 V) connected in series. Pressing the device with the hand, V_{oc} and I_{sc} can reach higher than ~ 50 V and ~ 5 μA , respectively. Fig. 7b shows the LEDs before and during hand's pressing on the FENG. The LEDs were simultaneously lit upon pressing (See Movie S3, Supporting Information). The results show that the mechanical energy harvesting ability of the FENG is capable of converting human motion to electrical energy, demonstrating the potential of the device to power wearable (or implantable) electronic devices. Another promising application of the developed FENG is self-powered touchscreens, which could be used in smart phones, tablets, E-ink papers, or touch-screen panels. As a step towards such implementations, we demonstrated the integration of the device with a 4-bit LCD screen, as illustrated in Fig. 7c. When gently tap the self-powered LCD screen by the user, the word PLAY is displayed on the screen without rectifiers or charging circuits (See Movie S4, Supporting Information). The biomechanical harvested energy (converted to electrical energy) allows for the letters to be displayed. The developed self-powered FENG-based display could increase the energy efficiency of smart phones and wearable devices by scavenging energy from the users' touch during regular operation thus reducing the frequency of required battery charges from external energy sources. Another

demonstration of the applicability of the FENG is on what can be considered as one of the most common, reliable, accessible and effective tools used for human-machine interfacing and information exchange: a keyboard [21]. We fabricated a flexible, foldable, and self-powered keyboard which converts the mechanical stimuli applied to the keyboard upon key-punching into an electric signal that is used to display the pressed letter on a computer monitor. The structural design and photograph of the thin film keyboard are shown in Fig. 7d and e, respectively. By using bar-coating technique (like the one shown in Fig. 5b), the top and bottom surface of a PPFE film is uniformly coated by electrically conductive paint without mask and with patterned shadow mask, respectively. The real-time keystroke tracing and recording is shown in Movie S5, Supporting Information. As the user types the word “SPARTANS”, the output is displayed (in real-time) on a computer monitor. The developed FENG-based keyboard can also be rolled (Fig. 7f) or folded (Fig. 7g) while keeping its functionality. This could offer a way to change today's large volume battery-operated keyboards into power-less portable devices that can be folded to the size of a business card.

4. Conclusion

In summary, we introduced a new type of energy harvesting method that takes advantage of ferroelectric phenomenon. Based on PPFE, we demonstrated the fabrication of lightweight, flexible, foldable, and biocompatible thin film FENG which is able to be power source for commercial electronics such as colorful LEDs. By adapting bar-coating technique, a large-area FENGs is fabricated. One of the compelling characteristics of FENG is that both of the V_{oc} and I_{sc} would be doubled with each folding of the FENG along an axis of symmetry, allowing the FENG to reach very high voltage if needed. Niche applications of FENGs are further demonstrated including a self-powered touching screen LCD which is capable of scavenging energy from users' touch, leading to vast prospect in today's abundant touch screen devices; and the flexible/foldable, self-powered keyboard which can be folded as business card size. Advantages such as lightweight, flexible, foldable, biocompatible, scalable, low cost and robustness could make FENG a promising and alternative method in the field of mechanical energy harvesting for various of autonomous electronics.

Acknowledgement

This work was supported by the National Science Foundation (NSF ECCS Award #1139773 (NSF CAREER Award) and #ECCS-1306311). The authors thank Composite Materials and Structures Center (CMSC) at Michigan State University, and Dr. P. Askeland for his assistance and suggestions. Finally, the authors are thankful to Dr. Le Cai from Prof. Wang's group (co-author) for productive discussions.

Appendix A. Supplementary material

Supplementary data associated with this article can be found in the online version at [http://dx.doi.org/S2211-2855\(16\)30424-4](http://dx.doi.org/S2211-2855(16)30424-4).

References

- S. Wang, Y. Xie, S. Niu, L. Lin, Z.L. Wang, Freestanding triboelectric-layer-based nanogenerators for harvesting energy from a moving object or human motion in contact and non-contact modes, *Adv. Mater.* 26 (2014) 2818–2824.
- H.-J. Kim, J.-H. Kim, K.-W. Jun, J.-H. Kim, W.-C. Seung, O.H. Kwon, J.-Y. Park, S.-W. Kim, I.-K. Oh, Silk nanofiber-networked bio-triboelectric generator: Silk Bio-TEG, *Adv. Energy Mater.* 6 (2016) 1502329.
- S. Wang, Z.-H. Lin, S. Niu, L. Lin, Y. Xie, K.C. Pradel, Z.L. Wang, Motion charged battery as sustainable flexible-power-unit, *ACS Nano* 7 (2013) 11263–11271.
- G. Zhu, Y.S. Zhou, P. Bai, X.S. Meng, Q. Jing, J. Chen, Z.L. Wang, A shape-adaptive thin-film-based approach for 50% high-efficiency energy generation through micro-grating sliding electrification, *Adv. Mater.* 26 (2014) 3788–3796.
- Y. Hu, Z.L. Wang, Recent progress in piezoelectric nanogenerators as a sustainable power source in self-powered systems and active sensors, *Nano Energy* 14 (2015) 3–14.
- S. Wang, L. Lin, Z.L. Wang, Triboelectric nanogenerators as self-powered active sensors, *Nano Energy* 11 (2015) 436–462.
- Z. Wen, J. Chen, M.-H. Yeh, H. Guo, Z. Li, X. Fan, T. Zhang, L. Zhu, Z.L. Wang, Blow-driven triboelectric nanogenerator as an active alcohol breath analyzer, *Nano Energy* 16 (2015) 38–46.
- Y. Yang, G. Zhu, H. Zhang, J. Chen, X. Zhong, Z.-H. Lin, Y. Su, P. Bai, X. Wen, Z.L. Wang, Triboelectric nanogenerator for harvesting wind energy and as self-powered wind vector sensor system, *ACS Nano* 7 (2013) 9461–9468.
- S. Lee, S.-H. Bae, L. Lin, Y. Yang, C. Park, S.-W. Kim, S.N. Cha, H. Kim, Y.J. Park, Z.L. Wang, Super-flexible nanogenerator for energy harvesting from gentle wind and as an active deformation sensor, *Adv. Funct. Mater.* 23 (2013) 2445–2449.
- J. Bae, J. Lee, S. Kim, J. Ha, B.-S. Lee, Y. Park, C. Choong, J.-B. Kim, Z.L. Wang, H.-Y. Kim, Flutter-driven triboelectrification for harvesting wind energy, *Nat. Commun.* 5 (2014) 4929.
- J. Chen, J. Yang, Z. Li, X. Fan, Y. Zi, Q. Jing, H. Guo, Z. Wen, K.C. Pradel, S. Niu, Networks of triboelectric nanogenerators for harvesting water wave energy: a potential approach toward blue energy, *ACS nano* 9 (2015) 3324–3331.
- W. Guo, X. Li, M. Chen, L. Xu, L. Dong, X. Cao, W. Tang, J. Zhu, C. Lin, C. Pan, Electrochemical cathodic protection powered by triboelectric nanogenerator, *Adv. Funct. Mater.* 24 (2014) 6691–6699.
- W. Tang, Y. Han, C.B. Han, C.Z. Gao, X. Cao, Z.L. Wang, Self-powered water splitting using flowing kinetic energy, *Adv. Mater.* 27 (2015) 272–276.
- G. Zhu, Y. Su, P. Bai, J. Chen, Q. Jing, W. Yang, Z.L. Wang, Harvesting water wave energy by asymmetric screening of electrostatic charges on a nanostructured hydrophobic thin-film surface, *ACS Nano* 8 (2014) 6031–6037.
- Y. Hu, C. Xu, Y. Zhang, L. Lin, R.L. Snyder, Z.L. Wang, A nanogenerator for energy harvesting from a rotating tire and its application as a self-powered pressure/speed sensor, *Adv. Mater.* 23 (2011) 4068–4071.
- L. Lin, Y. Hu, C. Xu, Y. Zhang, R. Zhang, X. Wen, Z.L. Wang, Transparent flexible nanogenerator as self-powered sensor for transportation monitoring, *Nano Energy* 2 (2013) 75–81.
- H. Zhang, Y. Yang, X. Zhong, Y. Su, Y. Zhou, C. Hu, Z.L. Wang, Single-electrode-based rotating triboelectric nanogenerator for harvesting energy from tires, *ACS Nano* 8 (2013) 680–689.
- T.-C. Hou, Y. Yang, H. Zhang, J. Chen, L.-J. Chen, Z.L. Wang, Triboelectric nanogenerator built inside shoe insole for harvesting walking energy, *Nano Energy* 2 (2013) 856–862.
- G. Zhu, P. Bai, J. Chen, Z.L. Wang, Power-generating shoe insole based on triboelectric nanogenerators for self-powered consumer electronics, *Nano Energy* 2 (2013) 688–692.
- P. Bai, G. Zhu, Z.-H. Lin, Q. Jing, J. Chen, G. Zhang, J. Ma, Z.L. Wang, Integrated multilayered triboelectric nanogenerator for harvesting biomechanical energy from human motions, *ACS Nano* 7 (2013) 3713–3719.
- J. Chen, G. Zhu, J. Yang, Q. Jing, P. Bai, W. Yang, X. Qi, Y. Su, Z.L. Wang, Personalized keystroke dynamics for self-powered human-machine interfacing, *ACS Nano* 9 (2015) 105–116.
- K.C. Pradel, W. Wu, Y. Ding, Z.L. Wang, Solution-derived ZnO homojunction nanowire films on wearable substrates for energy conversion and self-powered gesture recognition, *Nano Lett.* 14 (2014) 6897–6905.
- Y. Xie, S. Wang, S. Niu, L. Lin, Q. Jing, J. Yang, Z. Wu, Z.L. Wang, Grating-structured freestanding triboelectric-layer nanogenerator for harvesting mechanical energy at 85% total conversion efficiency, *Adv. Mater.* 26 (2014) 6599–6607.
- P. Bai, G. Zhu, Q. Jing, J. Yang, J. Chen, Y. Su, J. Ma, G. Zhang, Z.L. Wang, Membrane-based self-powered triboelectric sensors for pressure change detection and its uses in security surveillance and healthcare monitoring, *Adv. Funct. Mater.* 24 (2014) 5807–5813.
- C. Dagdeviren, B.D. Yang, Y. Su, P.L. Tran, P. Joe, E. Anderson, J. Xia, V. Doraiswamy, B. Dehdashti, X. Feng, Conformal piezoelectric energy harvesting and storage from motions of the heart, lung, and diaphragm, *Proc. Natl. Acad. Sci.* 111 (2014) 1927–1932.
- Q. Zheng, B. Shi, F. Fan, X. Wang, L. Yan, W. Yuan, S. Wang, H. Liu, Z. Li, Z.L. Wang, In vivo powering of pacemaker by breathing-driven implanted triboelectric nanogenerator, *Adv. Mater.* 26 (2014) 5851–5856.
- C. Dagdeviren, Y. Shi, P. Joe, R. Ghaffari, G. Balooch, K. Usgaonkar, O. Gur, P.L. Tran, J.R. Crosby, M. Meyer, Conformal piezoelectric systems for clinical and experimental characterization of soft tissue biomechanics, *Nat. Mater.* 14 (2015) 728–736.
- C. Dagdeviren, Y. Su, P. Joe, R. Yona, Y. Liu, Y.-S. Kim, Y. Huang, A.R. Damadoran, J. Xia, L.W. Martin, Conformable amplified lead zirconate titanate sensors with enhanced piezoelectric response for cutaneous pressure monitoring, *Nat. Commun.* 5 (2014) 4496.
- L. Persano, C. Dagdeviren, Y. Su, Y. Zhang, S. Girardo, D. Pisignano, Y. Huang, J.A. Rogers, High performance piezoelectric devices based on aligned arrays of nanofibers of poly(vinylidene fluoride-co-trifluoroethylene), *Nat. Commun.* 4 (2013) 1633.
- X. Pu, L. Li, M. Liu, C. Jiang, C. Du, Z. Zhao, W. Hu, Z.L. Wang, Wearable self-charging power textile based on flexible yarn supercapacitors and fabric nanogenerators, *Adv. Mater.* 28 (2016) 98–105.
- T. Zhou, C. Zhang, C.B. Han, F.R. Fan, W. Tang, Z.L. Wang, Woven structured triboelectric nanogenerator for wearable devices, *ACS Appl. Mater. Interfaces* 6 (2014) 14695–14701.
- C.K. Jeong, J. Lee, S. Han, J. Ryu, G.-T. Hwang, D.Y. Park, J.H. Park, S.S. Lee, M. Byun, S.H. Ko, A hyper-stretchable elastic-composite energy harvester, *Adv. Mater.* 27 (2015) 2866–2875.
- G.-T. Hwang, J. Yang, S.H. Yang, H.-Y. Lee, M. Lee, D.Y. Park, J.H. Han, S.J. Lee, C.K. Jeong, J. Kim, A reconfigurable rectified flexible energy harvester via solid-state single crystal grown PMN-PZT, *Adv. Energy Mater.* 5 (2015) 1500051.
- K.-I. Park, J.H. Son, G.-T. Hwang, C.K. Jeong, J. Ryu, M. Koo, I. Choi, S.H. Lee, M. Byun, Z.L. Wang, Highly-efficient, flexible piezoelectric pzt thin film nanogenerator on plastic substrates, *Adv. Mater.* 26 (2014) 2514–2520.
- G.-T. Hwang, Y. Kim, J.-H. Lee, S. Oh, C.K. Jeong, D.Y. Park, J. Ryu, H. Kwon, S.-G. Lee, B. Joung, Self-powered deep brain stimulation via a flexible pimnt energy harvester, *Energy Environ. Sci.* 8 (2015) 2677–2684.
- C. Wang, D. Hwang, Z. Yu, K. Takei, J. Park, T. Chen, B. Ma, A. Javey, User-interactive electronic skin for instantaneous pressure visualization, *Nat. Mater.* 12 (2013) 899–904.
- C. Wang, K. Takei, T. Takahashi, A. Javey, Carbon nanotube electronics—moving forward, *Chem. Soc. Rev.* 42 (2013) 2592–2609.
- L. Cai, S. Zhang, J. Miao, Z. Yu, C. Wang, Fully printed foldable integrated logic gates with tunable performance using semiconducting carbon nanotubes, *Adv. Funct. Mater.* 25 (2015) 5698–5705.
- C. Wang, J.-C. Chien, K. Takei, T. Takahashi, J. Nah, A.M. Niknejad, A. Javey, Extremely bendable, high-performance integrated circuits using semiconducting carbon nanotube networks for digital, analog, and radio-frequency applications, *Nano Lett.* 12 (2012) 1527–1533.
- J. Zhang, C. Wang, C. Zhou, Rigid/flexible transparent electronics based on separated carbon nanotube thin-film transistors and their application in display electronics, *ACS Nano* 6 (2012) 7412–7419.
- T. Takahashi, Z. Yu, K. Chen, D. Kiriyu, C. Wang, K. Takei, H. Shiraki, T. Chen, B. Ma, A. Javey, Carbon nanotube active-matrix backplanes for mechanically flexible visible light and x-ray imagers, *Nano Lett.* 13 (2013) 5425–5430.
- X. Pu, L. Li, H. Song, C. Du, Z. Zhao, C. Jiang, G. Cao, W. Hu, Z.L. Wang, A self-charging power unit by integration of a textile triboelectric nanogenerator and a flexible lithium-ion battery for wearable electronics, *Adv. Mater.* 27 (2015) 2472–2478.
- G.-T. Hwang, H. Park, J.-H. Lee, S. Oh, K.-I. Park, M. Byun, H. Park, G. Ahn, C.K. Jeong, K. No, Self-powered cardiac pacemaker enabled by flexible single crystalline PMN-PT piezoelectric energy harvester, *Adv. Mater.* 26 (2014) 4880–4887.
- C.K. Jeong, K.-I. Park, J.H. Son, G.-T. Hwang, S.H. Lee, D.Y. Park, H.E. Lee, H.K. Lee, M. Byun, K.J. Lee, Self-powered fully-flexible light-emitting system enabled by flexible energy harvester, *Energy Environ. Sci.* 7 (2014) 4035–4043.
- S. Kim, J.H. Son, S.H. Lee, B.K. You, K.-I. Park, H.K. Lee, M. Byun, K.J. Lee, Flexible crossbar-structured resistive memory arrays on plastic substrates via inorganic-based laser lift-off, *Adv. Mater.* 26 (2014) 7480–7487.
- C.-H. Wang, W.-S. Liao, Z.-H. Lin, N.-J. Ku, Y.-C. Li, Y.-C. Chen, Z.-L. Wang, C.-P. Liu, Optimization of the output efficiency of gan nanowire piezoelectric nanogenerators by tuning the free carrier concentration, *Adv. Energy Mater.* 4 (2014) 1400392.
- W. Wu, L. Wang, Y. Li, F. Zhang, L. Lin, S. Niu, D. Chenet, X. Zhang, Y. Hao, T.F. Heinz, Piezoelectricity of single-atomic-layer MoS₂ for energy conversion and piezotronics, *Nature* 514 (2014) 470–474.
- S. Xu, Y. Qin, C. Xu, Y. Wei, R. Yang, Z.L. Wang, Self-powered nanowire devices, *Nat. Nanotechnol.* 5 (2010) 366–373.
- J. Chen, G. Zhu, W. Yang, Q. Jing, P. Bai, Y. Yang, T.-C. Hou, Z.L. Wang, Harmonic-resonator-based triboelectric nanogenerator as a sustainable power source and a self-powered active vibration sensor, *Adv. Mater.* 25 (2013) 6094–6099.

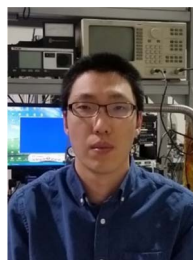
- [50] Y.S. Zhou, G. Zhu, S. Niu, Y. Liu, P. Bai, Q. Jing, Z.L. Wang, Nanometer resolution self-powered static and dynamic motion sensor based on micro-grated triboelectrification, *Adv. Mater.* 26 (2014) 1719–1724.
- [51] Z. Lin Wang, Triboelectric nanogenerators as new energy technology and self-powered sensors—principles, problems and perspectives, *Faraday Discuss.* 176 (2014) 447–458.
- [52] X. Li, Z.-H. Lin, G. Cheng, X. Wen, Y. Liu, S. Niu, Z.L. Wang, 3d fiber-based hybrid nanogenerator for energy harvesting and as a self-powered pressure sensor, *ACS Nano* 8 (2014) 10674–10681.
- [53] K.-I. Park, C.K. Jeong, J. Ryu, G.-T. Hwang, K.J. Lee, Flexible and large-area nanocomposite generators based on lead zirconate titanate particles and carbon nanotubes, *Adv. Energy Mater.* 3 (2013) 1539–1544.
- [54] M. Wegener, S. Bauer, Microstorms in cellular polymers: a route to soft piezoelectric transducer materials with engineered macroscopic dipoles, *ChemPhysChem* 6 (2005) 1014–1025.
- [55] S. Bauer, R. Gerhard-Mulhaupt, G.M. Sessler, Ferroelectrets: Soft electroactive foams for transducers, *Phys. Today* 57 (2004) 37–44.
- [56] J. Döring, V. Bovtun, M. Gaal, J. Bartusch, A. Erhard, M. Kreutzbruck, Y. Yakymenko, Piezoelectric and electrostrictive effects in ferroelectret ultrasonic transducers, *J. Appl. Phys.* 112 (2012) 084505.
- [57] Z. Luo, D. Zhu, J. Shi, S. Beeby, C. Zhang, P. Proynov, B. Stark, Energy harvesting using single and multilayer ferroelectret foams under compressive force, *IEEE Trans. Dielectr. Electr. Insul.* 22 (2015) 1360–1368.
- [58] K.-I. Park, M. Lee, Y. Liu, S. Moon, G.-T. Hwang, G. Zhu, J.E. Kim, S.O. Kim, D.K. Kim, Z.L. Wang, Flexible nanocomposite generator made of BaTiO₃ nanoparticles and graphitic carbons, *Adv. Mater.* 24 (2012) 2999–3004.
- [59] K.S. Ramadan, D. Sameoto, S. Ewoy, A review of piezoelectric polymers as functional materials for electromechanical transducers, *Smart Mater. Struct.* 23 (2014) 033001.
- [60] F.-C. Sun, A.M. Dongare, A.D. Asandei, S.P. Alpay, S. Nakhmanson, Temperature dependent structural, elastic, and polar properties of ferroelectric polyvinylidene fluoride (PVDF) and trifluoroethylene (TrFE) copolymers, *J. Mater. Chem. C* 3 (2015) 8389–8396.
- [61] Z. Liu, C. Pan, L. Lin, J. Huang, Z. Ou, Direct-write pvdf nonwoven fiber fabric energy harvesters via the hollow cylindrical near-field electrospinning process, *Smart Mater. Struct.* 23 (2013) 025003.
- [62] P. Pondrom, J. Hillenbrand, G.M. Sessler, J. Bös, T. Melz, Energy harvesting with single-layer and stacked piezoelectret films, *IEEE Trans. Dielectr. Electr. Insulation* 22 (2015) 1470–1476.
- [63] Y. Feng, K. Hagiwara, Y. Iguchi, Y. Suzuki, Trench-filled cellular parylene electret for piezoelectric transducer, *Appl. Phys. Lett.* 100 (2012) 262901.
- [64] J.-J. Wang, T.-H. Hsu, C.-N. Yeh, J.-W. Tsai, Y.-C. Su, Piezoelectric polydimethylsiloxane films for mems transducers, *J. Micromech. Microeng.* 22 (2011) 015013.
- [65] R. Yang, Y. Qin, L. Dai, Z.L. Wang, Power generation with laterally packaged piezoelectric fine wires, *Nat. Nanotechnol.* 4 (2009) 34–39.



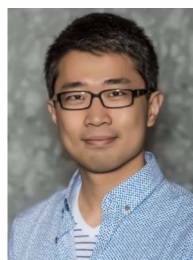
Wei Li received his B.S. and Ph.D. in Mechanical Engineering from Huazhong University of Science and Technology, China, in 2008 and 2013, respectively. He is currently a Ph.D. candidate at Michigan State University. From 2009 to 2011, he served as an R&D Engineer at National Lithography Tool Research and Development Center in Shanghai, where he contributed to the development of high-resolution step and scan optical lithography tools. His current research interests include smart materials for sensors, actuators, energy harvesters, ultra-precision positioning system, and active vibration/acoustic control. Dr. Li is a member of IEEE Robotics and Automation Society.



David Torres received his B.S. degree in Electrical and Computer Engineering from the University of Puerto Rico, Mayagüez, Puerto Rico in December 2012. He is currently working towards his Ph.D. degree in the Department of Electrical and Computer Engineering at Michigan State University. He participated in a number of research projects including; a summer research internship at MSU as an undergraduate and the Air Force Research Laboratories at Wright-Patterson Air Force Base, Dayton, OH as a graduate student. He has recently been awarded the Science, Mathematics And Research for Transformation (SMART) Scholarship for Service Program from the Department of Defense.



Tongyu Wang received his B.S. degree in Electrical and Computer Engineering from Beijing University of Aeronautics & Astronautics, Beijing, China, in July 2010. He is currently working towards his Ph.D. degree in the Department of Electrical and Computer Engineering, Michigan State University, East Lansing, MI, USA. He participated in numerous research and programs including: intern at Sony Mobile Communication AB, Beijing, China (2013), National Key Laboratory of Science & Technology on Inertia, Beijing, China (2010–2013), and Baocheng Aviation Instrument Co. Ltd., Baoji, China (2009). His research interests include development of smart materials-based MEMS devices and multilayer microfluidic systems.



Chuan Wang received his Ph.D. in Electrical Engineering from University of Southern California in 2011 and worked as a postdoctoral scholar in the department of Electrical Engineering and Computer Sciences at UC Berkeley from 2011 to 2013. He is currently an Assistant professor in the Electrical and Computer Engineering Department at Michigan State University. Dr. Wang's current research interests include: 1) Low-cost fully-printed flexible and stretchable electronics for displaying, sensing, and energy harvesting applications; and 2) High-performance nanoelectronics and optoelectronics using 2-dimensional semiconductors. He has published 41 journal papers with ~2500 citations and an h-index of 26.



Nelson Sepulveda received the B.S. degree in Electrical and Computer Engineering from the University of Puerto Rico, Mayagüez, Puerto Rico in 2001, and the M.S. and Ph.D. degrees in Electrical and Computer Engineering from Michigan State University, East Lansing, MI, USA, in 2002 and 2005, respectively. He has participated in several visiting faculty positions at the National Laboratories. He is currently an Associate Professor in the Electrical and Computer Engineering Department with a courtesy appointment in the Mechanical Engineering Department at Michigan State University. He is a recipient of the NSF CAREER (2010) and the MSU Teacher-Scholar Award (2015).